Elsevier Editorial System(tm) for Toxicon
Manuscript Draft

Manuscript Number:

Title: Margatoxin is a non-selective inhibitor of human Kv1.3 K+ channels

Article Type: Research Paper

Keywords: Margatoxin, MgTx, non-selective, Kv1.3, Kv1.2

Corresponding Author: Prof. Gyorgy Panyi, MD PhD

Corresponding Author's Institution: University of Debrecen, Medical and Health Science Center

First Author: Adam Bartok

Order of Authors: Adam Bartok; Agnes Toth, Ph.D.; Sandor Somodi, M.D., Ph.D.; Tibor G Szanto, Ph.D.; Peter Hajdu, Ph.D.; Gyorgy Panyi, MD PhD; Zoltan Varga, Ph.D.

Abstract: During the last few decades many short-chain peptides have been isolated from the venom of different scorpion species. These toxins inhibit a variety of K+ channels by binding to and plugging the pore of the channels from the extracellular side thereby inhibiting ionic fluxes through the plasma membrane. The high affinity and selectivity of some toxins promote these peptides to become lead compounds for potential therapeutic use.
Voltage-gated K+ channels can be classified into several families based on their gating properties and sequence homology. Members of a given family may have high sequence similarity, such as Kv1.1, Kv1.2 and Kv1.3 channels, therefore selective inhibitors of one specific channel are quite rare. The lack of selectivity of such peptides and the inhibition of more types of channels might lead to undesired side effects upon therapeutic application or may lead to incorrect conclusion regarding the role of a particular ion channel in a physiological or pathophysiological response either in vitro or in vivo.
Margatoxin (MgTx) is often considered as a high affinity and selective inhibitor of the Kv1.3 channel. MgTx consists of 39 amino acids stabilized by 3 disulfide bridges isolated from the venom of the scorpion Centruroides margaritatus. This peptide is widely used in ion channel research, however, a comprehensive study of its selectivity with electrophysiological methods has not been published yet. Using the patch-clamp technique we conducted a comprehensive assessment of the selectivity of MgTx. Measurements were carried out on L929 cells expressing mKv1.1 channels, human peripheral lymphocytes expressing Kv1.3 channels and transiently transfected tsA201 cells with the following ion channels: hKv1.1, hKv1.2, hKv1.3, hKv1.4-IR, hKv1.5, hKv1.6, hKv1.7, rKv2.1, Shaker-IR, hERG, hKCa1.1, hKCa3.1 and hNav1.5. Margatoxin is indeed high affinity inhibitor of Kv1.3 channel (Kd = 11.7 pM) but is not selective, since it inhibits the Kv1.2 channel with even higher affinity (Kd = 6.4 pM) and Kv1.1 in the nanomolar range (Kd = 4.2 nM).
Based on our comprehensive data MgTX has to be considered a non-selective Kv1.3 inhibitor, and thus, experiments aiming at elucidating the significance of Kv1.3 in in vitro or in vivo physiological responses have to be carefully evaluated.

Suggested Reviewers: Lourival Possani Ph.D.
Professor, Instituto de Biotecnologia UNAM, Departamento de Medicina Molecular y Bioprocesos
possani@ibt.unam.mx
Internationally recognized expert in scorpion toxins

Heike Wulff Ph.D.
Associate Professor, Department of Pharmacology, University of California, Davis
hwulff@ucdavis.edu
international expert in Kv1.3 pharmacology

Christine Beeton Ph.D.
Assistant Professor, Department of Molecular Physiology and Biophysics, Baylor College of Medicine
beeton@bcm.edu
international expert in Kv1.3 pharmacology

Ildiko Szabo Ph.D.
Associate Professor, Department of Biology, University of Padova
ildi@bio.unipd.it
internationally recognized expert in the physiological role of ion channels in the immune system

Bernard Attali Ph.D.
Professor, Dept of Physiology & Pharmacology, Sackler Medical School, Tel Aviv University
battali@post.tau.ac.il
internationally recognized expert in ion channel pharmacology,biophysics and neurobiology

Ricardo Rodriguez de la Vega Ph.D.
research fellow, Université Paris-Sud
ricardo.rodriguezdelavega@gmail.com
international expert in toxins

Opposed Reviewers:

Title page

Margatoxin is a non-selective inhibitor of human Kv1.3 K^+ channels

Adam Bartok[a], Agnes Toth[a], Sandor Somodi[b], Tibor G. Szanto[a], Peter Hajdu[c], Gyorgy Panyi[a,d], Zoltan Varga[a]

[a] Department of Biophysics and Cell Biology, University of Debrecen, Faculty of Medicine
98. Nagyerdei krt., Debrecen, Hungary, 4032
Adam Bartok: adam.bartok@gmail.com
Agnes Toth: agi.toth@yahoo.com
Tibor Szanto G: szantogt@freemail.hu
Gyorgy Panyi: panyi@med.unideb.hu
Zoltan Varga: veze@med.unideb.hu

[b] Division of Metabolic Diseases, Department of Internal Medicine, University of Debrecen
98. Nagyerdei krt., Debrecen, Hungary, 4032
Sandor Somodi: somodi.s.dr@gmail.com

[c] Department of Biophysics and Cell Biology, University of Debrecen, Faculty of Dentistry
98. Nagyerdei krt., Debrecen, Hungary, 4032
Peter Hajdu: hajdup@med.unideb.hu

[d] MTA-DE Cell Biology and Signaling Research Group
4032 Debrecen, Egyetem tér 1.

Send correspondence to:

Gyorgy Panyi, M.D., Ph.D.
University of Debrecen, Faculty of Medicine
Department of Biophysics and Cell Biology

98. Nagyerdei krt.
Debrecen
Hungary
4032

phone: (+36)(52) 412-623 (Dept. secretary)
(+36-52) 411-600 x65617 (through operator)
(+36-52) 411-717 x65617 (through automatic switchboard)

fax: (+36)(52)532-201
email: panyi@med.unideb.hu
http://biophys.med.unideb.hu/en/node/311

Abstract

Margatoxin (MgTx), an alpha-KTx scorpion toxin, is considered a selective inhibitor of the Kv1.3 K+ channel. This peptide is widely used in ion channel research; however, a comprehensive study of its selectivity with electrophysiological methods has not been published yet. The lack of selectivity might lead to undesired side effects upon therapeutic application or may lead to incorrect conclusion regarding the role of a particular ion channel in a physiological or pathophysiological response either *in vitro* or *in vivo*.

Using the patch-clamp technique we characterized the selectivity profile of MgTx using L929 cells expressing mKv1.1 channels, human peripheral lymphocytes expressing Kv1.3 channels and transiently transfected tsA201 cells expressing hKv1.1, hKv1.2, hKv1.3, hKv1.4-IR, hKv1.5, hKv1.6, hKv1.7, rKv2.1, Shaker-IR, hERG, hKCa1.1, hKCa3.1 and hNav1.5 channels. MgTx is indeed a high affinity inhibitor of Kv1.3 (Kd = 11.7 pM) but is not selective, it inhibits the Kv1.2 channel with similar affinity (Kd = 6.4 pM) and Kv1.1 in the nanomolar range (Kd = 4.2 nM).

Based on our comprehensive data MgTX has to be considered a non-selective Kv1.3 inhibitor, and thus, experiments aiming at elucidating the significance of Kv1.3 in *in vitro* or in vivo physiological responses have to be carefully evaluated.

Keywords: Margatoxin, MgTx, non-selective, Kv1.3, Kv1.2

[1]1. Introduction

Peptide toxins isolated from animal venoms are well known blockers of the pore of plasma membrane ion channels thereby inhibiting cellular functions including action potential generation, proliferation and differentiation (Jimenez-Vargas et al., 2012; Pedraza Escalona and Possani, 2013; Rodriguez de la Vega and Possani, 2004, 2005). This property may allow the therapeutic application of such molecules in various diseases such as asthma, cardiac arrhythmia, hypertension and T-cell mediated autoimmune diseases (Bergeron and Bingham, 2012; Chandy et al., 2004; Jimenez-Vargas et al., 2012; Panyi et al., 2006) or obesity and insulin resistance (Upadhyay et al., 2013).

K^+ channels play a key role in the regulation of the membrane potential of excitable and non-excitable cells (Abbott, 2006; Korn and Trapani, 2005; Varga et al., 2010; Varga et al., 2011). Kv1.3 is a voltage-gated K^+ channel, which is expressed in a variety of cells and tissues e.g. in the central nervous system, pancreatic islets, lymphocytes, etc. (Gutman et al., 2005). Interestingly, Kv1.3 is the dominant voltage-gated K^+ channel of human T-lymphocytes and its expression is sensitively regulated during terminal differentiation of these cells (Wulff et al., 2003). For example, effector memory T cells (T_{EM}) generated by repeated chronic antigen stimuli express a high number of Kv1.3 as compared to other K^+ channels and their proliferation becomes exclusively sensitive to Kv1.3 inhibitors (Wulff et al., 2003). As T_{EM} cells are responsible for the tissue damage in chronic autoimmune diseases, such as Multiple Sclerosis and Rheumatoid Arthritis, the therapeutic application of Kv1.3 blockers for the inhibition of T_{EM} proliferation is imminent and well-supported in animal models of these diseases (Chi et al., 2012; Panyi et al., 2006).

Kv1.x channels share high sequence homology and tend to form functional heterotetrameric structures in different tissues. Kv1.2 is one of the channels having the highest similarity to Kv1.3. Kv1.2 is

[1] Non-standard abbreviations: rMgTx: recombinant margatoxin (Alomone Labs, Jerusalem, Israel, cat. No.: RTM-325, Lot: MA103); sMgTx: synthetic margatoxin (Peptide Institute Inc. Osaka, Japan, cat. No.: 4290-s, Lot: 560914)

primarily expressed in the central and peripheral nervous system forming homotetramers or associated with other Kv1.x channel subunits (Coleman et al., 1999; Dodson et al., 2003). Several natural peptide toxins show high affinity to Kv1.3 but also block Kv1.2 channels e.g. Css20, Anuroctoxin, Noxiustoxin and Charybdotoxin (Bagdany et al., 2005; Corzo et al., 2008; Grissmer et al., 1994). Highly selective blockers of Kv1.3 are rarely isolated directly from animal venoms (but see Vm24 (Varga et al., 2012)), however, with site-directed mutations selective peptides can be constructed, as was demonstrated for ShK-170 (Pennington et al., 2009), Mokatoxin-1 (Takacs et al., 2009) and OSK1-20 (Mouhat et al., 2005).

Margatoxin (MgTx) is a 39 amino-acid-long peptide stabilized by 3 disulfide bridges with a molecular weight of 4185, isolated from the venom of the scorpion *Centruroides margaritatus.* (Garcia-Calvo et al., 1993) This peptide is widely used in the field of ion channel research (Kalman et al., 1998; Koch et al., 1997). Margatoxin is considered as a high affinity and selective inhibitor of the Kv1.3 channel (Jang et al., 2011; Kazama et al., 2012; Toldi et al., 2013; Zhao et al., 2013) however, a comprehensive study of its selectivity with electrophysiological methods has not been published yet. When MgTx was isolated and its high affinity interaction with Kv1.3 was precisely characterized it was only tested on a limited number of channels excluding Kv1.1, Kv1.2 and Kv1.4 channels, those with high sequence homology to Kv1.3 (Garcia-Calvo et al., 1993). Later the authors who described MgTx and other workgroups refer to the peptide as potent blocker of Kv1.1, Kv1.2 and Kv1.3 channels (Anangi et al., 2012; Koch et al., 1997; Suarez-Kurtz et al., 1999; Vianna-Jorge et al., 2003) whereas the references do not describe or contain any information about the interaction of MgTx and the Kv1.1 or Kv1.2 channels. In the absence of the selectivity profile of MgTx results from radioactively labeled MgTx binding assays or the biological effect of the peptide as a direct proof of Kv1.3 expression is not fully straightforward (Arkett et al., 1994; Li et al., 2008; Saria et al., 1998). In addition, MgTx shares high sequence homology with other scorpion peptides that block both Kv1.3 and Kv1.2 channels with high affinity (Noxiustoxin, Css20) suggesting that MgTx may be a non-selective peptide as well.

We conducted electrophysiological measurements with the patch-clamp technique in voltage-clamp mode to test the selectivity of MgTx. Measurements were carried out on L929 cells expressing mKv1.1 channels, human peripheral lymphocytes expressing Kv1.3 channels and tsA201 cells transiently transfected with the following ion channels: hKv1.1, hKv1.2, hKv1.3, hKv1.4-IR, hKv1.5, hKv1.6, hKv1.7, rKv2.1, Shaker-IR, hERG, hKCa1.1, hKCa3.1 and hNav1.5. Our results indicate that MgTx is not a highly selective inhibitor of Kv1.3 channels as had been assumed in several previous studies.

2. Materials and methods

2.1 Sequence alignments

To obtain amino acid sequences of the toxins the NCBI protein database was used then for the alignment of the sequences the built-in blastp (protein-protein BLAST) algorithm was used.

2.2 Chemicals

Recombinant margatoxin (rMgTx) was purchased from Alomone Labs, (Jerusalem, Israel, cat. No.: RTM-325, Lot: MA103). Synthetic margatoxin (sMgTx) was obtained from Peptide Institute Inc. (Osaka, Japan, cat. No.: 4290-s, Lot: 560914). Other chemicals were obtained from Sigma-Aldrich Kft, Budapest, Hungary.

2.3 Cells

tsA201 cells, derived from HEK-293 (Shen et al., 1995) were grown under standard conditions, as described previously (Corzo et al., 2008). Human peripheral lymphocytes were obtained from healthy volunteers. Mononuclear cells were isolated using Ficoll-Hypaque density gradient separation technique and cultured in 24-well culture plates in a 5% CO_2 incubator at 37°C in RPMI 1640 medium supplemented

with 10% fetal calf serum (Sigma-Aldrich), 100 µg/ml penicillin, 100 µg/ml streptomycin, and 2 mM L-glutamine (density, 5 x 10^5 cells per ml) for 2 to 5 days. 5, 7.5 or 10 µg/ml phytohemagglutinin A (Sigma-Aldrich) was added to the medium to increase K^+ channel expression. L929 cells stably expressing mKv1.1 channel have been described earlier (Grissmer et al., 1994) and were kind gifts from Dr. Heike Wulff (University of California, Davis, Davis, CA).

2.4 Heterologous expression of ion channels

tsA201 cells were transiently transfected with Ca^{2+} phosphate transfection kit (Sigma-Aldrich, Hungary) according to the manufacturer's instructions with the following channel coding vectors: hKv1.1, hKv1.2, hKv1.6 and hKv1.7 pCMV6-GFP plasmid (OriGene Technologies, Rockville, MD). hKv1.3 (previously cloned into p-EGFP-C1 vector from pRc-CMV2 plasmid, kind gift from C. Deutsch, University of Pennsylvania, Philadelphia, PA), hKv1.4-IR (inactivation ball deletion mutant) in pcDNA3 vector (kind gift from D. Fedida, University of British Columbia, Vancouver, Canada), hKv1.5 in pEYFP vector (kind gift from A. Felipe, University of Barcelona, Barcelona, Spain), rKv2.1 (gift from S. Korn, University of Connecticut, Storrs, CT), Shaker-IR (inactivation ball deletion mutant) (gift from G. Yellen, Harvard Medical School, Boston, MA), hKv11.1 (hERG, kind gift from SH. Heinemann, Max-Plank-Gesellschaft, Jena, Germany), KCa1.1 in pClneo vector (kind gift from T. Hoshi, University of Pennsylvania, Philadelphia, PA), hKCa3.1 in pEGFP-C1 vector (gift from H. Wulff, University of California, Davis CA) and hNav1.5 (gift from R. Horn, Thomas Jefferson University, Philadelphia, PA). hKv1.4-IR, rKv2.1, Shaker-IR, hERG, KCa3.1 and Nav1.5 coding vectors were co-transfected with a plasmid coding green fluorescent protein (GFP) gene in a molar ratio of 10:1. Currents were recorded 24 or48 h after transfection. Positive transfectants were identified with Nikon TE2000U or TS100 fluorescence microscope (Nikon, Tokyo, Japan). The hKv1.2 expression vector coding sequence (Origene RG222200) was confirmed by sequencing using the following primers: Forward1: AGCTCGTTTAGTGAACCGTCA, Reverse1: TGCTGTTGGAATAGGTGTGG,

Forward2: TTTCGGGAAGATGAAGGCTA, Reverse2: AGGAGGCCCAATTCTCTCAT, Forward3: TCCAGACACTCCAAAGGTC, Reverse3: CTCTCGTCGCTCTCCATCTC.

2.5 Electrophysiology

Measurements were carried out using patch-clamp technique in voltage-clamp mode. Whole cell currents were recorded on lymphocytes and L929 cells. Transfected tsA201 cells were studied in the outside-out configuration of patch-clamp. For the recordings Axon Axopatch 200A and 200B amplifiers and Axon Digidata 1200 and 1440 digitizers were used (Molecular Devices, Sunnyvale, CA). Micropipettes were pulled from GC 150 F-15 borosilicate capillaries (Harvard Apparatus Kent, UK) resulting in 3- to 5-MΩ resistance in the bath solution. For most of the measurements the bath solution consisted of 145 mM NaCl, 5 mM KCl, 1 mM $MgCl_2$, 2.5 mM $CaCl_2$, 5.5 mM glucose, 10 mM HEPES, pH 7.35. For the measurements of hKv11.1 (hERG) channels the extracellular solution contained 5 mM KCl, 10 mM HEPES, 20 mM glucose, 2 mM $CaCl_2$, 2 mM $MgCl_2$, 0.1 mM $CdCl_2$, 140 mM choline-chloride, pH 7.35. Bath solutions were supplemented with 0.1 mg/ml BSA when MgTx was dissolved in different concentrations. The measured osmolarity of the extracellular solutions was between 302 and 308 mOsM/L. Generally the pipette solution contained 140 mM KF, 2 mM $MgCl_2$, 1 mM $CaCl_2$, 10 mM HEPES and 11 mM EGTA, pH 7.22. To measure Kv11.1 channels the intracellular solution consisted of 140 mM KCl, 10 mM HEPES, 2mM $MgCl_2$ and 10 mM EGTA, pH 7.22, for the KCa3.1 recordings it contained 150 mM K-aspartate, 5mM HEPES, 10 mM EGTA, 8.7 mM $CaCl_2$, 2 mM $MgCl_2$, pH 7.22 resulting in 1 µM free Ca^{2+} in the solution to activate KCa3.1 channels fully (Grissmer et al., 1993). To measure KCa1.1 the intracellular solution contained 140 mM KCl, 10 mM EGTA, 9.69 mM $CaCl_2$, 5 mM HEPES, pH 7.22 thus giving 5 µM free Ca^{2+} concentration to allow the activation of KCa1.1 channels at moderate membrane depolarization (Avdonin et al., 2003). The osmolarity of the pipette filling solutions was 295 mOsM/L.

To measure hKv1.1, hKv1.2, hKv1.3, hKv1.4, hKv1.5, hKv1.6, hKv1.7, Shaker and rKv2.1 currents 15 to 50 ms long depolarization impulses were applied to +50 mV from a holding potential of -100 mV every 15 or 30 s. For hKv11.1 channels, currents were evoked with a voltage step from a holding potential of -80 mV to +20 mV followed by a step to -40 mV, during the latter the peak current was measured. Pulses were delivered every 30 s. For KCa1.1 channels, a voltage step to +50 mV was preceded by a 10-ms hyperpolarization to -120 mV from a holding potential of 0 mV every 15 s. KCa3.1 currents were elicited every 15 s with voltage ramps to +50 mV from a holding potential of -100 mV. Nav1.5 currents were measured by applying depolarization pulses to 0 mV from a holding potential of -120 mV every 15s.

To acquire and analyze the measured data pClamp9/10 software package was used. Current traces were lowpass-filtered by the analog four-pole Bessel filters of the amplifiers. The sampling frequency was 2-50 kHz, at least twice the filter cut-off frequency. The effect of the toxins in a given concentration was determined as remaining current fraction ($RF = I/I_0$, where I_0 is the peak current in the absence of the toxin and I is the peak current at equilibrium block at a given toxin concentration). Points on the dose-response curves represent the mean of 3-8 independent measurements where the error bars represent the S.E.M. Data points were fitted with a two-parameter Hill equation, $RF = Kd^H/(Kd^H+[Tx]^H)$, where Kd is the dissociation constant, H is the Hill coefficient and [Tx] is the toxin concentration. To estimate Kd from two toxin concentrations we used the Lineweaver-Burk analysis, where 1/RF was plotted as a function of toxin concentration and fitting a straight line to the points, where Kd = 1/slope.

3. Results

3.1 Endogenous currents in tsA-201 cells

Figure 1A shows that whole-cell clamped non-transfected tsa201 cells display an endogenous voltage-gated outward current with an activation threshold of ~–20 mV. The magnitude of this current was determined using depolarizing pulses to +50 mV from a holding potential of -100 mV (Fig. 1B). The mean current amplitude was 337.1 pA (N = 16, S.E.M. = 48.5 pA). Application of 1nM recombinant MgTx (rMgTx, Alomone Labs) in the extracellular solution did not inhibit the whole-cell endogenous current (RF=0.98, S.E.M.=0.01, Fig. 1C). Figs. 1A and 1B also shows that the endogenous current significantly decreased upon excising a patch to outside-out configuration (11.6 pA, N = 9, S.E.M. = 0.8 pA). The box plots representing the distribution of the peak currents recorded in whole-cell and excised outside-out configuration are shown in Fig. 1D. Although the endogenous current is MgTx insensitive, measurements on transfected tsA201 cells were always carried out in outside-out patch configuration thereby decreasing the relevance of the endogenous current as background during recordings from heterologously expressed channels.

3.2 Selectivity profile of MgTx

Since high affinity toxins block K^+ channels in the picomolar range, the effect of 1nM rMgTx on the different ion channels was tested to assess MgTx selectivity. Outside-out patch-clamp recordings of currents in the absence and presence of 1nM rMgTx are shown if Fig. 2A-N for hKv1.1 (A), hKv1.2 (B), hKv1.3 (C) hKv1.4 (D) hKv1.5 (E) hKv1.6 (F) hKv1.7 (G) rKv2.1 (H) hKv11.1 (I) Shaker IR (J) hKCa3.1 (K), hKCa1.1 (L) hNav1.5 (M) and mKv1.1 (N). Significant blocking effect of rMgTx was observed on both murine and human Kv1.1, as well as hKv1.2 and hKv1.3 channels (Fig. 2A, B, C, N). Despite the high sequence homology rMgTx had no significant effect on hKv1.4, hKv1.5, hKv1.6, hKv1.7 channels (Fig. 2D-

G, nor on any of the additional channels tested in this study such as rKv2.1, Shaker, hKv11.1, hKCa3.1, hKCa1.1 and hNav1.5 channels (Fig. 2H-M). Remaining current fractions at 1 nM rMgTX concentration are summarized in Fig. 2O.

The three ion channel types, which were inhibited by 1 nM rMgTX were further studied to obtain a more accurate rank order and potency of MgTx. Due to the low affinity block of hKv1.1 channels, a complete dose-response curve would have required very large quantities of rMgTx. Therefore we used the remaining current fractions at two measured concentrations to estimate the Kd values for mKv1.1 and hKv1.1 To this end we applied the Lineweaver-Burk analysis to obtain Kd values of 1.7 nM and 4.2 nM, respectively (Fig. 3A). The significantly higher affinity of rMgTx for hKv1.2 and hKv1.3 allowed the construction of a full dose-response relationship and the determination of the Kd values from the Hill equation. The protocols for obtaining the peak currents were identical to those in Fig. 2B and C, for hKv1.2 and hKv1.3, respectively. We found that rMgTx blocks hKv1.2 and hKv1.3 channels with Kd = 6.4 pM and 11.7 pM respectively (Fig. 3B), the Hill coefficients were close to 1 in both cases. Fig. 3C shows that rMgTx blocks the hKv1.3 current quickly and reversibly, equilibrium block develops in ~ 1 min. following the start of the perfusion with toxin-containing solution (gray bar, 100 pM MgTx) and full recovery of the peak currents is in ~7 min. upon perfusing the recording chamber with toxin-free solution. On the contrary, the block of the hKv1.2 current (Fig. 3D) develops on a much slower time-course and perfusion of the recording chamber with toxin-free medium results in very slow partial recovery from block. In the latter case cumulative dose-response relationships could not be obtained, thus, each point in the Fig. 3B was obtained from independent experiments for both hKv1.3 and hKv1.2 for comparable results.

For quality assurance of our data, we have performed two additional sets of experiments, both aiming at confirming the pharmacological activity of the rMgTx. First, the potency of rMgTx was confirmed in inhibiting the endogenous Kv1.3 channels expressed in activated human T lymphocytes. Fitting the dose-

response relationship using the Hill equation resulted in Kd = 10.1 pM (Fig. 4A), in good agreement with previous data on the inhibition of endogenous or heterologously expressed Kv1.3 and our previously published results (Toth et al., 2009). Second, we have characterized the inhibition of hKv1.2 and hKv1.3 currents by MgTx obtained from a different source to rule out the possibility of peptide production error. Fig. 4B shows high affinity block of hKv1.2 and hKv1.3 by synthetic MgTx (sMgTx), Kd = 14.3 pM and Kd = 12.0 pM were obtained, respectively. Thus sMgTx and rMgTx block hKv1.2 and hKv1.3 channels with similar affinities. High affinity block of Kv1.3 channels by sMgTx was also observed in activated lymphocytes (Kd = 22.8 pM, data not shown).

4. Discussion

We aimed to screen the effect of MgTx on several different ion channels using the same methods and expression system for a reliable comparison of the results. We therefore chose the easy to perform transient expression technique in the widely used tsA201 cell line. First, we tested the tsA201 cells for the presence of endogenous currents as these currents may interfere with the interpretation of pharmacological experiments designed to characterize the heterologously expressed channels. As reported earlier HEK-293 cells express various ion channels endogenously (He and Soderlund, 2010; Jiang et al., 2002; Varghese et al., 2006; Yu and Kerchner, 1998; Zhu et al., 1998). Similarly, we recorded whole-cell outward currents evoked by depolarizing pulses in tsA201 cells, however, the current measured on outside-out patches was negligible. Although the endogenous current was insensitive to 1 nM rMgTx (Fig. 1C) and the overexpression of the channels may eliminate the contribution of the endogenous background current to the whole cell current, we chose overexpression and excised outside-out patch-clamp (see Figs. 1A, B and D) to minimize the potential errors in the pharmacological data.

Using such a recording configuration we tested the following ion channels: hKv1.1, hKv1.2, hKv1.3, hKv1.4-IR, hKv1.5, hKv1.6, hKv1.7, rKv2.1, Shaker-IR, hKv11.1 (hERG), hKCa1.1, hKCa3.1 and hNav1.5. We only found a significant blocking effect on hKv1.1, hKv1.2 and hKv1.3 channels. Our results show picomolar dissociation constants for hKv1.2 and hKv1.3 and nanomolar Kd for hKv1.1. An earlier study found rat Kv1.6 channels to be sensitive to MgTx (Kd = 5 nM) (Garcia-Calvo et al., 1993), however, we did not find a significant effect of 1 nM MgTx on human Kv1.6 channels (Fig. 2F). We confirmed these results on hKv1.2 and hKv1.3 channels using MgTx from an additional source. Synthetic MgTx blocked Kv1.2 and Kv1.3 channels expressed in tsA201 cells with values similar to those obtained with rMgTx confirming the comparable affinities for the two channels.

285 The inhibition of mKv1.1 current in stably transfected L929 cell line was slightly higher than that of
286 human Kv1.1 measured in tsA201 cells. The difference in the Kd values may be due to the different
287 expression systems and the different availability of possible interacting partners of the channel in tsA201
288 and L929 cells or the difference in the primary structure of mKv1.1 and hKv1.1 channels (Coetzee et al.,
289 1999). The affinities of MgTx for hKv1.2 and hKv1.3 are quite similar; however, the kinetics of the block
290 (Fig. 3C, D) suggests that the mode of association and dissociation of MgTx to the two receptors is
291 different. Equilibrium block for Kv1.3 developed faster and this block was reversible upon perfusing the
292 cells with toxin-free bath solution, whereas block kinetics for Kv1.2 were much slower and the blocking
293 effect was only partially reversible or irreversible. We previously found similar blocking features for
294 another peptide toxin, Css20, which has very high amino acid sequence identity with MgTx (76%) and has
295 similar pharmacological properties as well. With docking simulations we identified the most likely
296 interacting residue pairs between Css20 and the Kv1.2 and Kv1.3 channels. We propose that MgTx
297 probably interacts mostly with the selectivity filter of Kv1.3 by plugging it with the K28 lysine residue and
298 prefers contact with the turret and axially located residues of Kv1.2 via a hydrogen bonding network
299 (Corzo et al., 2008).
300
301 Blast analysis (Blastp algorithm, NCBI) of the amino acid sequence of MgTx shows the highest similarity
302 to known, non-selective inhibitors of the Kv1.3 channel, such as Hongotoxin 1 (90%) (Koschak et al.,
303 1998), Noxiustoxin (79%) (Grissmer et al., 1994) and Css20 (76%) (Corzo et al., 2008) (Table 1.). These
304 toxins inhibit both Kv1.2 and Kv1.3 channels with similar affinities. Known Kv1.3 selective toxins based on
305 the definition of Giangiacomo (where at least a 100-fold difference between the Kd values of the toxin
306 on a given channel is observed)(Giangiacomo et al., 2004), exhibit much lower sequence identity with
307 MgTx such as OSK1 (61%) (Mouhat et al., 2005), Kaliotoxin (58%) (Grissmer et al., 1994) and Vm24 (45%)
308 (Varga et al., 2012).

Based on solely the primary structure of the peptide and sequence homology with other peptides one cannot make accurate conclusions about the selectivity of a peptide toxin. However, the high similarity of the residues may suggest a similar 3D structure, and consequently the biological effect of the peptides may be also similar. Toxins in this group of similar peptides were isolated from different scorpion species, however, all belonging to the same genus *Centruroides,* indicating that the toxins have the same evolutional origin. Additionally, MgTx shows high sequence homology to other toxins isolated from other species belonging to the genus *Centruroides* (ClTx1 and ClTx2 from *C. limpidus limpidus*, Ce1, Ce2, Ce4 and Ce5 from *C. elegans*), but the effect of these toxins on both Kv1.2 and Kv1.3 channels has not been determined yet.

Well known, highly Kv1.3 selective toxins exhibit lower sequence identities with MgTx and are isolated from various scorpion genera. Based on this data it can be assumed that toxins of species of genus *Centruroides* possess common residues that allow the inhibition of more Kv1.x channels, therefore screening the effect of MgTx on especially Kv1.x channels can provide us valuable information about the residues that determine the receptor specificity of the peptide.

In vivo studies of Kv1.3 blocker peptide toxins clearly show their potential in suppressing T-cell mediated inflammatory reactions (Tarcha et al., 2012; Varga et al., 2012). In such experiments selectivity of the toxin is crucial to avoid potential side effects by blocking other Kv1.X channels. Kv1.1 was shown to be expressed in neurons (Gutman et al., 2005; Sinha et al., 2006; Wang et al., 1994), differentiating chondrocytes (Varga et al., 2011) in the distal convoluted tubule in the kidney (San-Cristobal et al., 2013) in bone marrow-derived human mesenchymal stem cells (You et al., 2013). Importance of Kv1.1 expression in the nervus vagus in cardiac function was shown in mice (Glasscock et al., 2010) and the channel is involved in the glucose-stimulated insulin release in β-cells (Ma et al., 2011). Kv1.2 is expressed in different neurons (Bakondi et al., 2008; Fulton et al., 2011; Rusznak et al., 2008; Utsunomiya et al., 2008; Wang et al., 1994) and the malfunction of both Kv1.1 and Kv1.2 channels were

shown to cause cerebellar ataxia (Browne et al., 1994; Xie et al., 2010). Consequently, the use of Kv1.3 inhibitors with poor selectivity may alter the physiological functions mentioned above. For example, continuous, 8-day application of MgTx *in vivo* in minipigs caused hypersalivation and decrease of appetite (Koo et al., 1997). This effect may be due to the inhibition of Kv1.1 or Kv1.2 channels expressed in neurons involved in the regulation of salivation and the sensation of appetite.

Our results show that MgTx inhibits hKv1.2 and hKv1.3 with high affinity in the picomolar range and both human and murine Kv1.1 in the nanomolar range, consequently if MgTx receptors are found on a given cell or tissue even with the confirmation of the presence of Kv1.3 in the plasma membrane with western blot, confocal microscopy etc., identification of other MgTx receptors such as Kv1.1 and Kv1.2 channels may be missed. Therefore the use of MgTx in such experiments must be reconsidered.

5. Acknowledgements

This research was supported by TÁMOP 4.2.4. A/2-11-1-2012-0001 'National Excellence Program', TÁMOP 4.2.2-A-11/1/KONV-2012-0025, TÁMOP-4.2.2/B-10/1-2010-0024 and OTKA K 75904 and OTKA NK 101337. Peter Hajdu is supported by Lajos Szodoray Fellowship. The technical assistance of Ms. Cecilia Nagy is highly appreciated.

Fig. 1, Bartok et al.

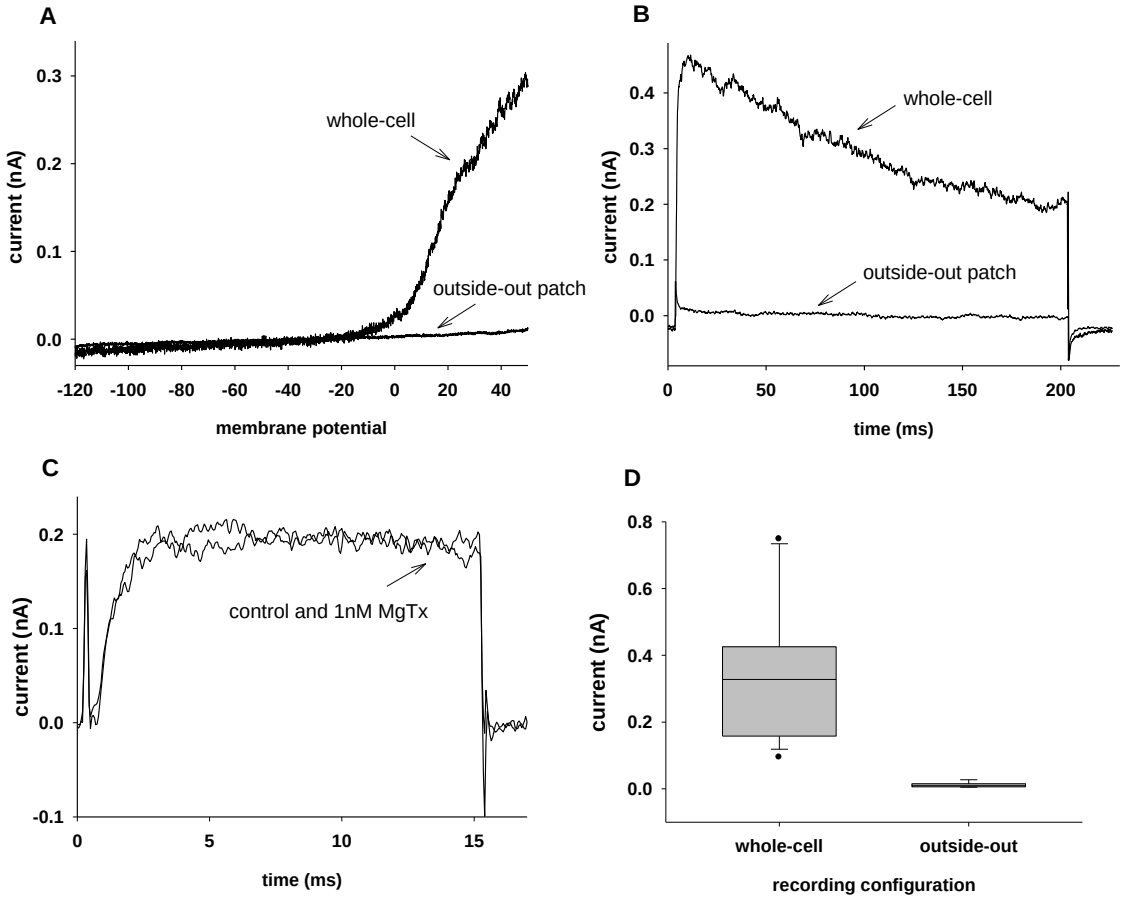

Figure 1. Voltage-gated outward endogenous currents in non-transfected tsA201 cells.

Currents were evoked using a voltage ramp protocol **(A)** ranging from -120 mV to +50 mV in 200ms or using a 200-ms-long voltage step protocol to +50 mV **(B)** in either whole cell configuration or following the excision of patches to outside out configuration (as indicated). The holding potential was −100 mV. **(C)** Whole-cell endogenous currents were evoked by 15-ms-long pulses to +50 mV from a holding potential of −100 mV before (control) and during the perfusion of the recording chamber with 1nM MgTx containing bath solution. 1 nM MgTx did not inhibit the whole-cell endogenous currents. **(D)** Box and whiskers plot of the endogenous currents in non-transfected tsa201 cells in whole cell and in excised outside out patch configuration. Peak currents were determined from current traces evoked as in panel B (N=17 and N=9 for whole-cell and outside-out configuration, respectively). Horizontal lines indicate the medians, the boxes indicate 25-75 percentile of the data whereas whiskers and dots indicate 10-90 percentile and the outliers, respectively.

Fig. 2, Bartok et al.

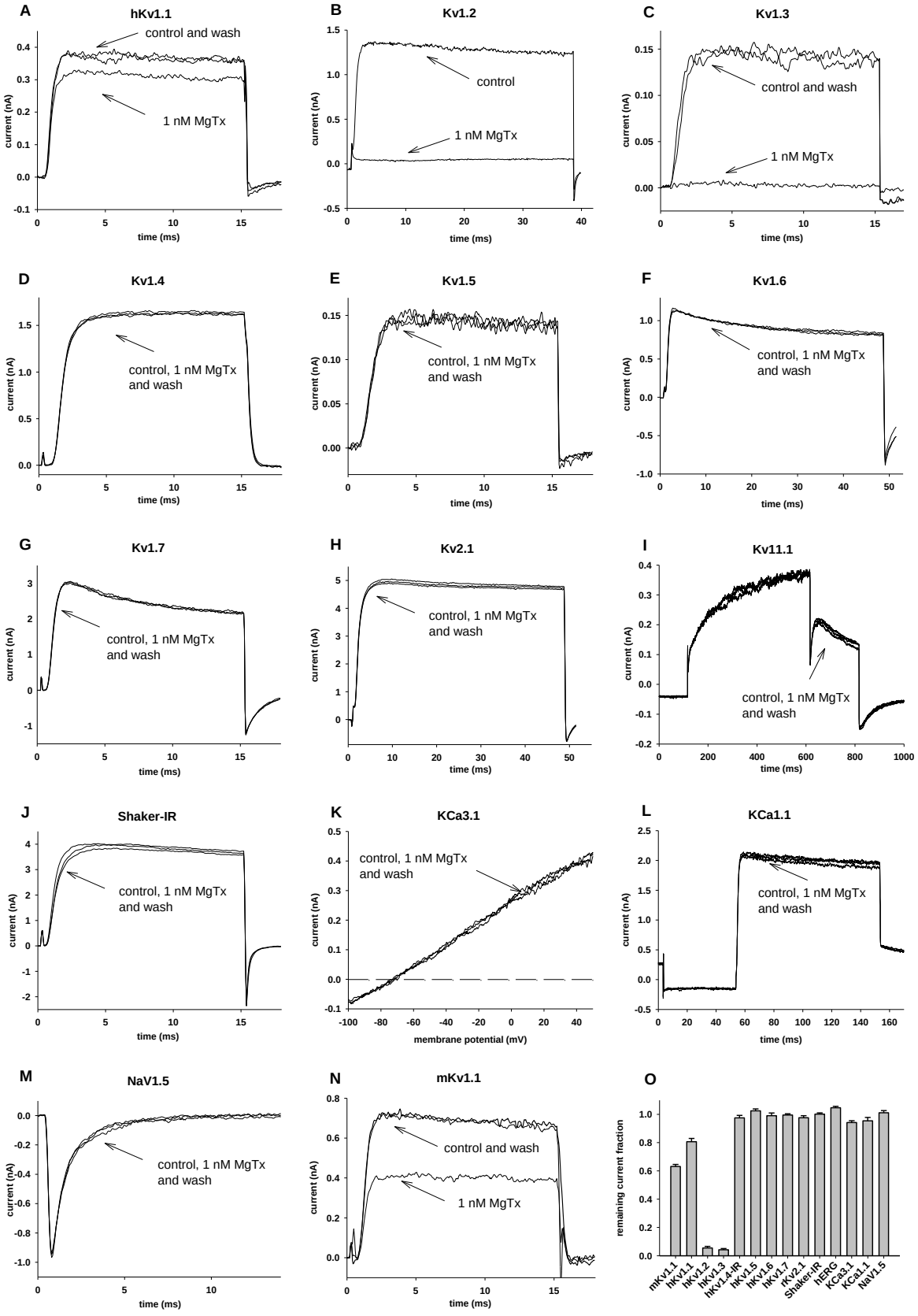

Legends to Fig 2

Figure 2. Selectivity profile of MgTx.

Effect of 1 nM MgTx was assayed on outside out patches excised from tsA201 cells transfected with different ion channel genes **(A-M)** and on L929 cells stably expressing mKv1.1 channels **(N)**. Representative traces show the currents measured in the bath solution before the application of MgTx (control), after reaching equilibrium block upon application of 1 nM MgTx (1 nM MgTx) and after recovering from the block applying toxin free bath solution in the perfusion system (wash out). Traces were 3-point boxcar filtered. **(A-H, J, N)** currents were evoked from holding potentials of −100 mV by depolarizations to +50 mV for durations ranging from 15 ms to 50 ms as indicated on the panels. The time between depolarizing pulses was 15 s (panel labels go here with 15 ipi) or 30 s (panel labels go here with 15 ipi). hKv11.1 **(I)** currents were measured with a voltage step from a holding potential of -80 mV to +20 mV followed by a step to -40 mV, during the latter the peak current was measured. Pulses were delivered every 30 s. For hKCa1.1 **(L)** channels, a voltage step to +50 mV was preceded by a 10-ms hyperpolarization to -120 mV from a holding potential of 0 mV every 15 s. hKCa3.1 **(K)** currents were elicited every 15 s with voltage ramps to +50 mV from a holding potential of -120 mV. hNav1.5 **(M)** currents were measured by applying depolarization pulses to 0 mV from a holding potential of -120 mV every 15 s. **(O)** The effect of 100 pM and 1 nM MgTx on the peak currents was reported as the remaining current fraction (RF = I/I_0, where I_0 is the peak current in the absence of the toxin and I is the peak current at equilibrium block at a given toxin concentration). Bars represent the mean of 3-8 independent measurements, error bars indicate the S.E.M. MgTx blocked hKv1.1, mKv1.1, hKv1.2 and hKv1.3 channels at the applied concentrations.

Fig. 3, Bartok et al.

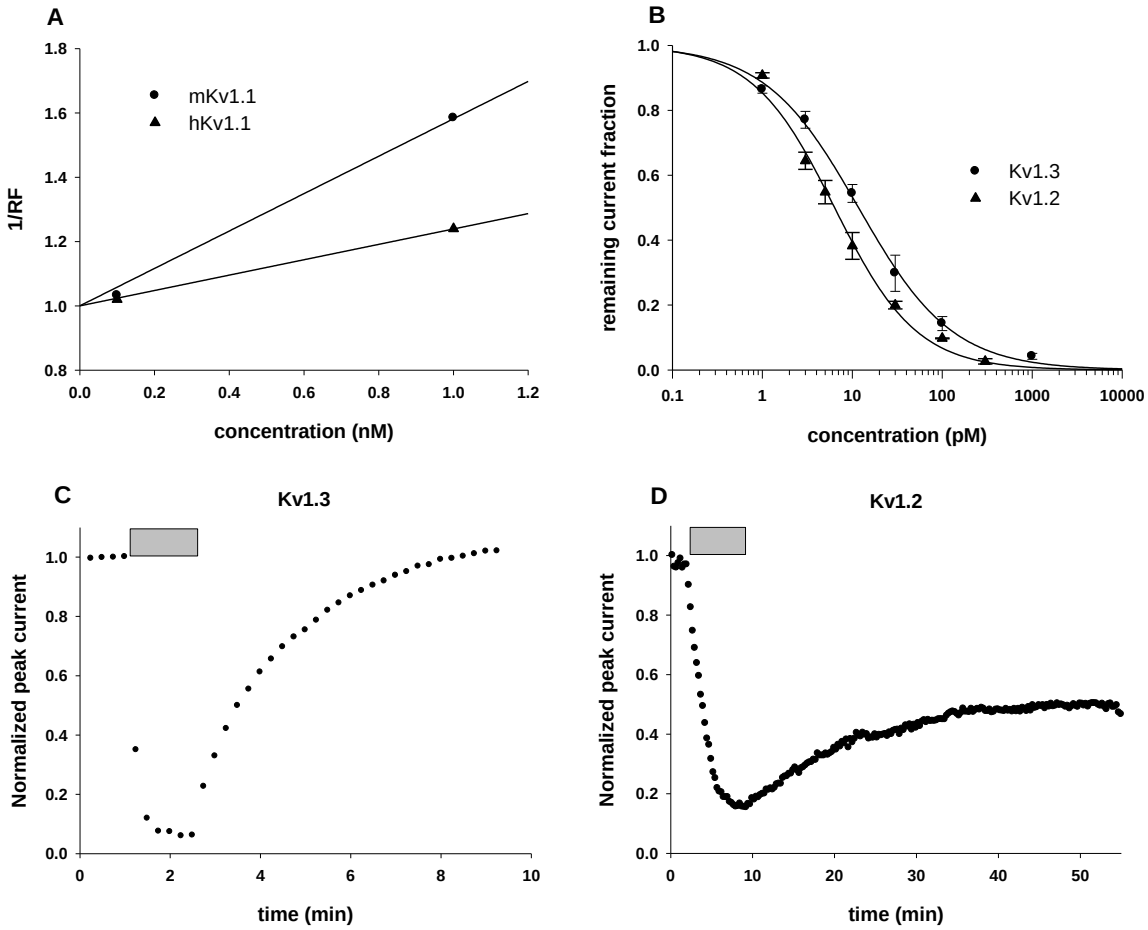

Figure 3. Block of Kv1.1, Kv1.2 and Kv1.3 currents by MgTx.

Peak currents were determined using protocols and experimental conditions as in Fig. 2. The effect of the toxins at a given concentration was determined as remaining current fraction (RF = I/I_0, where I_0 is the peak current in the absence of the toxin and I is the peak current at equilibrium block at a given toxin concentration) **(A)** Concentration dependence of the block of murine and human Kv1.1 channels by MgTx. Kd was determined from the Lineweaver-Burk analysis, where the reciprocal of the remaining current fraction (1/RF) is plotted as a function of toxin concentration and fitting a line to the data points yields Kd = 1/slope assuming 1:1 channel-toxin stoichiometry. Kd = 1.72 nM for mKv1.1 and Kd = 4.18 nM

for hKv1.1 was obtained from the fits. **(B)** High affinity, concentration dependent block of Kv1.2 and Kv1.3 channels by MgTx. Points on the dose-response curves represent the mean of 3-8 independent measurements where the error bars represent the S.E.M. Data points were fitted with a two-parameter Hill equation, $RF = Kd^H/(Kd^H+[Tx]^H)$, where Kd is the dissociation constant, H is the Hill coefficient and [Tx] is the toxin concentration. The best fit yielded Kd = 6.35 pM, H = 0.95 for Kv1.2 and Kd = 11.73 pM, H = 0.83 for Kv1.3. **(C, D)** Normalized peak currents measured in outside-out patch configuration on tsA201 cells expressing Kv1.3 **(C)** or Kv1.2 **(D)** channels and plotted as a function of time as 100 pM MgTx was applied to the bath solution (gray bars) and then removed from the extracellular medium. Pulses were delivered every 15 s. Perfusion with toxin-free medium resulted in very slow partial recovery from block in case of Kv1.2 **(D)**.

413 **Fig. 4., Bartok et al.**
414

415

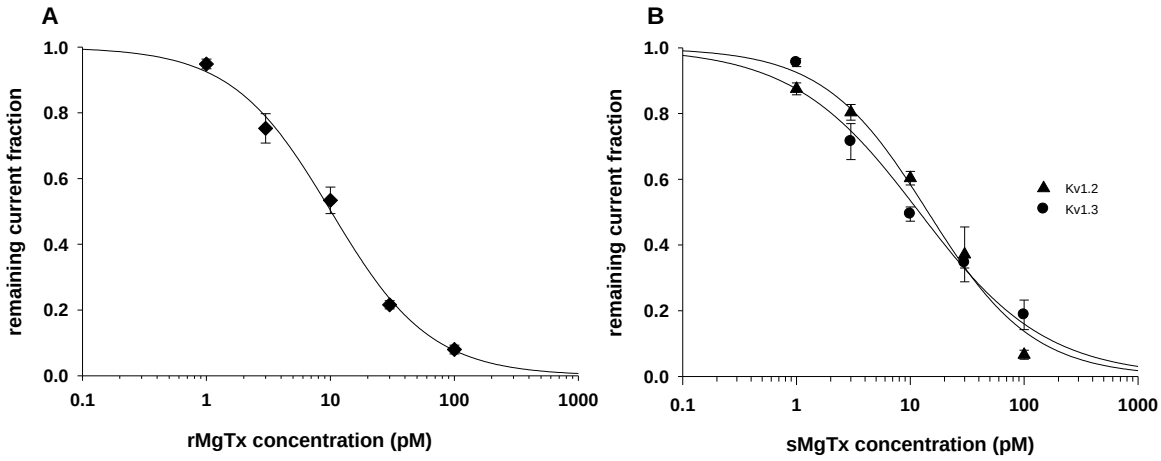

416

417

418 **Figure 4. Reference measurements to confirm the pharmacological effects of MgTx**

419 **(A)** Concentration dependence of the block of human T lymphocyte Kv1.3 channels by recombinant
420 MgTx (rMgTx). Whole-cell Kv1.3 currents were recorded in human peripheral blood T cells using voltage
421 protocols as for Fig 2 C. Remaining current fraction was determined at various toxin concentrations as in
422 described in the legends to Fig. 3. Points on the dose-response curves represent the mean of 3-5
423 independent measurements where the error bars represent the S.E.M. Data points were fitted with a
424 two-parameter Hill equation, $RF = Kd^H/(Kd^H+[Tx]^H)$, where Kd is the dissociation constant, H is the Hill
425 coefficient and [Tx] is the toxin concentration. The best fit yielded Kd = 22.8 pM and H = 1.1. **(B)**
426 Concentration dependence of the block of hKv1.2 and hKv1.3 channels by synthetic MgTx (sMgTx).
427 Channels were expressed in tsa201 cells, outside-out patch currents were recorded using protocols and
428 experimental conditions as for Fig 2 B (hKv1.2) and C (hKv1.3). The calculation of remaining current
429 fraction and the construction of the dose-response curve were as in Fig 4A for n = 3-5 independent
430 experiments at each toxin concentration. The best fit yielded Kd = 14.3 pM, H = 0.94 for Kv1.2 and Kd =
431 12 pM, H = 0.8 for Kv1.3.

Tables

Table 1

A

toxin name	species	sequence	Query cover	Max identity	Accession	Kd Kv1.2 (nM)	Kd Kv1.3 (nM)	Kd $_{Kv1.2}$ / Kd $_{Kv1.3}$
MgTx	*Centruroides margaritatus*	TIINVKCTSPKQCLPPCKAQFGQSAGAKCMNGKCKCYPH	100%	100%	P40755.1			
Hongotoxin 1	*Centruroides limbatus*	TVIDVKCTSPKQCLPPCKAQFGIRAGAKCMNGKCKCYPH	100%	90%	P59847.1	0.07	0.09	0.78
Noxiustoxin	*Centruroides noxius*	TIINVKCTSPKQCSKPCKELYGSSAGAKCMNGKCKCYNN	100%	79%	P08815.3	2	1	2.00
Css20	*Centruroides suffusus suffusus*	IFINVKCSSPQQCLKPCKAAFGISAGGKCINGKCKCYP-	97%	76%	P85529.1	1.26	7.21	0.17

B

toxin name	species	sequence	Query cover	Max identity	Accession	Kd Kv1.2 (nM)	Kd Kv1.3 (nM)	Kd $_{Kv1.2}$ / Kd $_{Kv1.3}$
MgTx	*Centruroides margaritatus*	-TIINVKCTSPKQCLPPCKAQFGQSAGAKCMNGKCKCYPH	100%	100%	P40755.1			
OSK1	*Orthochirus scrobiculosus*	GVIINVKCKISRQCLEPCK-KAGMRFG-KCMNGKCHCTPK	79%	61%	P55896.1	5.4	0.014	385.71
Kaliotoxin	*Androctonus mauritanicus*	GVEINVKCSGSPQCLKPCK-DAGMRFG-KCMNRKCHCTP-	92%	58%	AAB20997.1	>1000	0.65	>1538.46
Vm24	*Vaejovis mexicanus smithi*	--AAAISCVGSPECPPKCR-AQGCKNG-KCMNRKCKCYYC	84%	45%	P0DJ31.1	5-10	0.0029	>1724.14

Footnote to table 1: Sequence analysis (Blastp algorithm, NCBI) of MgTx. (A) Amino acid sequence of toxins with known affinities for Kv1.2 and Kv1.3 in decreasing identity % order. MgTx shows the highest similarity to known, non-selective inhibitors of Kv1.3 channel, such as Hongotoxin 1, Noxiustoxin and Css20. (B) Amino acid sequence of toxins wit high selectivity for Kv1.3 over Kv1.2. Kv1.3 selective toxins OSK1, Kaliotoxin and Vm24 show much lower sequence identity with MgTx. In the tables we indicate the common name of the peptides, the scorpion species from those the peptides were isolated, and the full amino acid sequences of the peptides including the database accession numbers. The similarity is represented by the query cover, which gives the percent of the query length that is included in the aligned sequences and the maximum identity, the percent similarity between the query and subject sequences over the length of the coverage area. Kd (or IC50) values on Kv1.2 and Kv1.3 channels are shown in nM. For the values the following references were used: Hongotoxin1 (Koschak et al., 1998), Noxiustoxin (Grissmer et al., 1994), Css20 (Corzo et al., 2008), OSK1 (Mouhat et al., 2005), Kaliotoxin (Grissmer et al., 1994), Vm24 (Varga et al., 2012). The ratio of Kd values (Kd $_{Kv1.2}$ / Kd $_{Kv1.3}$) measures the selectivity of the peptides to Kv1.3 channel (Giangiacomo et al., 2004).

6. References:

Abbott, G.W., 2006. Molecular mechanisms of cardiac voltage-gated potassium channelopathies. Curr Pharm Des 12, 3631-3644.

Anangi, R., Koshy, S., Huq, R., Beeton, C., Chuang, W.J., King, G.F., 2012. Recombinant expression of margatoxin and agitoxin-2 in Pichia pastoris: an efficient method for production of KV1.3 channel blockers. PLoS One 7, e52965.

Arkett, S.A., Dixon, J., Yang, J.N., Sakai, D.D., Minkin, C., Sims, S.M., 1994. Mammalian osteoclasts express a transient potassium channel with properties of Kv1.3. Receptors Channels 2, 281-293.

Avdonin, V., Tang, X.D., Hoshi, T., 2003. Stimulatory action of internal protons on Slo1 BK channels. Biophys J 84, 2969-2980.

Bagdany, M., Batista, C.V., Valdez-Cruz, N.A., Somodi, S., Rodriguez de la Vega, R.C., Licea, A.F., Varga, Z., Gaspar, R., Possani, L.D., Panyi, G., 2005. Anuroctoxin, a new scorpion toxin of the alpha-KTx 6 subfamily, is highly selective for Kv1.3 over IKCa1 ion channels of human T lymphocytes. Mol Pharmacol 67, 1034-1044.

Bakondi, G., Por, A., Kovacs, I., Szucs, G., Rusznak, Z., 2008. Voltage-gated K+ channel (Kv) subunit expression of the guinea pig spiral ganglion cells studied in a newly developed cochlear free-floating preparation. Brain Res 1210, 148-162.

Bergeron, Z.L., Bingham, J.P., 2012. Scorpion toxins specific for potassium (K+) channels: a historical overview of peptide bioengineering. Toxins (Basel) 4, 1082-1119.

Browne, D.L., Gancher, S.T., Nutt, J.G., Brunt, E.R., Smith, E.A., Kramer, P., Litt, M., 1994. Episodic ataxia/myokymia syndrome is associated with point mutations in the human potassium channel gene, KCNA1. Nat Genet 8, 136-140.

475 Chandy, K.G., Wulff, H., Beeton, C., Pennington, M., Gutman, G.A., Cahalan, M.D., 2004. K+ channels as
476 targets for specific immunomodulation. Trends Pharmacol Sci 25, 280-289.
477 Chi, V., Pennington, M.W., Norton, R.S., Tarcha, E.J., Londono, L.M., Sims-Fahey, B., Upadhyay, S.K.,
478 Lakey, J.T., Iadonato, S., Wulff, H., Beeton, C., Chandy, K.G., 2012. Development of a sea anemone toxin
479 as an immunomodulator for therapy of autoimmune diseases. Toxicon 59, 529-546.
480 Coetzee, W.A., Amarillo, Y., Chiu, J., Chow, A., Lau, D., McCormack, T., Moreno, H., Nadal, M.S., Ozaita,
481 A., Pountney, D., Saganich, M., Vega-Saenz de Miera, E., Rudy, B., 1999. Molecular diversity of K+
482 channels. Ann N Y Acad Sci 868, 233-285.
483 Coleman, S.K., Newcombe, J., Pryke, J., Dolly, J.O., 1999. Subunit composition of Kv1 channels in human
484 CNS. J Neurochem 73, 849-858.
485 Corzo, G., Papp, F., Varga, Z., Barraza, O., Espino-Solis, P.G., Rodriguez de la Vega, R.C., Gaspar, R., Panyi,
486 G., Possani, L.D., 2008. A selective blocker of Kv1.2 and Kv1.3 potassium channels from the venom of the
487 scorpion Centruroides suffusus suffusus. Biochem Pharmacol 76, 1142-1154.
488 Dodson, P.D., Billups, B., Rusznak, Z., Szucs, G., Barker, M.C., Forsythe, I.D., 2003. Presynaptic rat Kv1.2
489 channels suppress synaptic terminal hyperexcitability following action potential invasion. J Physiol 550,
490 27-33.
491 Fulton, S., Thibault, D., Mendez, J.A., Lahaie, N., Tirotta, E., Borrelli, E., Bouvier, M., Tempel, B.L.,
492 Trudeau, L.E., 2011. Contribution of Kv1.2 voltage-gated potassium channel to D2 autoreceptor
493 regulation of axonal dopamine overflow. J Biol Chem 286, 9360-9372.
494 Garcia-Calvo, M., Leonard, R.J., Novick, J., Stevens, S.P., Schmalhofer, W., Kaczorowski, G.J., Garcia, M.L.,
495 1993. Purification, characterization, and biosynthesis of margatoxin, a component of Centruroides
496 margaritatus venom that selectively inhibits voltage-dependent potassium channels. J Biol Chem 268,
497 18866-18874.

Giangiacomo, K.M., Ceralde, Y., Mullmann, T.J., 2004. Molecular basis of alpha-KTx specificity. Toxicon 43, 877-886.

Glasscock, E., Yoo, J.W., Chen, T.T., Klassen, T.L., Noebels, J.L., 2010. Kv1.1 potassium channel deficiency reveals brain-driven cardiac dysfunction as a candidate mechanism for sudden unexplained death in epilepsy. J Neurosci 30, 5167-5175.

Grissmer, S., Nguyen, A.N., Aiyar, J., Hanson, D.C., Mather, R.J., Gutman, G.A., Karmilowicz, M.J., Auperin, D.D., Chandy, K.G., 1994. Pharmacological characterization of five cloned voltage-gated K+ channels, types Kv1.1, 1.2, 1.3, 1.5, and 3.1, stably expressed in mammalian cell lines. Mol Pharmacol 45, 1227-1234.

Grissmer, S., Nguyen, A.N., Cahalan, M.D., 1993. Calcium-activated potassium channels in resting and activated human T lymphocytes. Expression levels, calcium dependence, ion selectivity, and pharmacology. J Gen Physiol 102, 601-630.

Gutman, G.A., Chandy, K.G., Grissmer, S., Lazdunski, M., McKinnon, D., Pardo, L.A., Robertson, G.A., Rudy, B., Sanguinetti, M.C., Stuhmer, W., Wang, X., 2005. International Union of Pharmacology. LIII. Nomenclature and molecular relationships of voltage-gated potassium channels. Pharmacol Rev 57, 473-508.

He, B., Soderlund, D.M., 2010. Human embryonic kidney (HEK293) cells express endogenous voltage-gated sodium currents and Na v 1.7 sodium channels. Neurosci Lett 469, 268-272.

Jang, S.H., Choi, S.Y., Ryu, P.D., Lee, S.Y., 2011. Anti-proliferative effect of Kv1.3 blockers in A549 human lung adenocarcinoma in vitro and in vivo. Eur J Pharmacol 651, 26-32.

Jiang, B., Sun, X., Cao, K., Wang, R., 2002. Endogenous Kv channels in human embryonic kidney (HEK-293) cells. Mol Cell Biochem 238, 69-79.

Jimenez-Vargas, J.M., Restano-Cassulini, R., Possani, L.D., 2012. Toxin modulators and blockers of hERG K(+) channels. Toxicon 60, 492-501.

522 Kalman, K., Pennington, M.W., Lanigan, M.D., Nguyen, A., Rauer, H., Mahnir, V., Paschetto, K., Kem,
523 W.R., Grissmer, S., Gutman, G.A., Christian, E.P., Cahalan, M.D., Norton, R.S., Chandy, K.G., 1998. ShK-
524 Dap22, a potent Kv1.3-specific immunosuppressive polypeptide. J Biol Chem 273, 32697-32707.
525 Kazama, I., Maruyama, Y., Murata, Y., Sano, M., 2012. Voltage-dependent biphasic effects of chloroquine
526 on delayed rectifier K(+)-channel currents in murine thymocytes. J Physiol Sci 62, 267-274.
527 Koch, R.O., Wanner, S.G., Koschak, A., Hanner, M., Schwarzer, C., Kaczorowski, G.J., Slaughter, R.S.,
528 Garcia, M.L., Knaus, H.G., 1997. Complex subunit assembly of neuronal voltage-gated K+ channels. Basis
529 for high-affinity toxin interactions and pharmacology. J Biol Chem 272, 27577-27581.
530 Koo, G.C., Blake, J.T., Talento, A., Nguyen, M., Lin, S., Sirotina, A., Shah, K., Mulvany, K., Hora, D., Jr.,
531 Cunningham, P., Wunderler, D.L., McManus, O.B., Slaughter, R., Bugianesi, R., Felix, J., Garcia, M.,
532 Williamson, J., Kaczorowski, G., Sigal, N.H., Springer, M.S., Feeney, W., 1997. Blockade of the voltage-
533 gated potassium channel Kv1.3 inhibits immune responses in vivo. J Immunol 158, 5120-5128.
534 Korn, S.J., Trapani, J.G., 2005. Potassium channels. IEEE Trans Nanobioscience 4, 21-33.
535 Koschak, A., Bugianesi, R.M., Mitterdorfer, J., Kaczorowski, G.J., Garcia, M.L., Knaus, H.G., 1998. Subunit
536 composition of brain voltage-gated potassium channels determined by hongotoxin-1, a novel peptide
537 derived from Centruroides limbatus venom. J Biol Chem 273, 2639-2644.
538 Li, Y.F., Zhuo, Y.H., Bi, W.N., Bai, Y.J., Li, Y.N., Wang, Z.J., 2008. Voltage-gated potassium channel Kv1.3 in
539 rabbit ciliary epithelium regulates the membrane potential via coupling intracellular calcium. Chin Med J
540 (Engl) 121, 2272-2277.
541 Ma, Z., Lavebratt, C., Almgren, M., Portwood, N., Forsberg, L.E., Branstrom, R., Berglund, E., Falkmer, S.,
542 Sundler, F., Wierup, N., Bjorklund, A., 2011. Evidence for presence and functional effects of Kv1.1
543 channels in beta-cells: general survey and results from mceph/mceph mice. PLoS One 6, e18213.

544 Mouhat, S., Visan, V., Ananthakrishnan, S., Wulff, H., Andreotti, N., Grissmer, S., Darbon, H., De Waard,
545 M., Sabatier, J.M., 2005. K+ channel types targeted by synthetic OSK1, a toxin from Orthochirus
546 scrobiculosus scorpion venom. Biochem J 385, 95-104.
547 Panyi, G., Possani, L.D., Rodriguez de la Vega, R.C., Gaspar, R., Varga, Z., 2006. K+ channel blockers: novel
548 tools to inhibit T cell activation leading to specific immunosuppression. Curr Pharm Des 12, 2199-2220.
549 Pedraza Escalona, M., Possani, L.D., 2013. Scorpion beta-toxins and voltage-gated sodium channels:
550 interactions and effects. Front Biosci 18, 572-587.
551 Pennington, M.W., Beeton, C., Galea, C.A., Smith, B.J., Chi, V., Monaghan, K.P., Garcia, A., Rangaraju, S.,
552 Giuffrida, A., Plank, D., Crossley, G., Nugent, D., Khaytin, I., Lefievre, Y., Peshenko, I., Dixon, C., Chauhan,
553 S., Orzel, A., Inoue, T., Hu, X., Moore, R.V., Norton, R.S., Chandy, K.G., 2009. Engineering a stable and
554 selective peptide blocker of the Kv1.3 channel in T lymphocytes. Mol Pharmacol 75, 762-773.
555 Rodriguez de la Vega, R.C., Possani, L.D., 2004. Current views on scorpion toxins specific for K+-channels.
556 Toxicon 43, 865-875.
557 Rodriguez de la Vega, R.C., Possani, L.D., 2005. Overview of scorpion toxins specific for Na+ channels and
558 related peptides: biodiversity, structure-function relationships and evolution. Toxicon 46, 831-844.
559 Rusznak, Z., Bakondi, G., Pocsai, K., Por, A., Kosztka, L., Pal, B., Nagy, D., Szucs, G., 2008. Voltage-gated
560 potassium channel (Kv) subunits expressed in the rat cochlear nucleus. J Histochem Cytochem 56, 443-
561 465.
562 San-Cristobal, P., Lainez, S., Dimke, H., de Graaf, M.J., Hoenderop, J.G., Bindels, R.J., 2013. Ankyrin-3 is a
563 novel binding partner of the voltage-gated potassium channel Kv1.1 implicated in renal magnesium
564 handling. Kidney Int.
565 Saria, A., Seidl, C.V., Fischer, H.S., Koch, R.O., Telser, S., Wanner, S.G., Humpel, C., Garcia, M.L., Knaus,
566 H.G., 1998. Margatoxin increases dopamine release in rat striatum via voltage-gated K+ channels. Eur J
567 Pharmacol 343, 193-200.

568 Shen, E.S., Cooke, G.M., Horlick, R.A., 1995. Improved expression cloning using reporter genes and
569 Epstein-Barr virus ori-containing vectors. Gene 156, 235-239.
570 Sinha, K., Karimi-Abdolrezaee, S., Velumian, A.A., Fehlings, M.G., 2006. Functional changes in genetically
571 dysmyelinated spinal cord axons of shiverer mice: role of juxtaparanodal Kv1 family K+ channels. J
572 Neurophysiol 95, 1683-1695.
573 Suarez-Kurtz, G., Vianna-Jorge, R., Pereira, B.F., Garcia, M.L., Kaczorowski, G.J., 1999. Peptidyl inhibitors
574 of shaker-type Kv1 channels elicit twitches in guinea pig ileum by blocking kv1.1 at enteric nervous
575 system and enhancing acetylcholine release. J Pharmacol Exp Ther 289, 1517-1522.
576 Takacs, Z., Toups, M., Kollewe, A., Johnson, E., Cuello, L.G., Driessens, G., Biancalana, M., Koide, A.,
577 Ponte, C.G., Perozo, E., Gajewski, T.F., Suarez-Kurtz, G., Koide, S., Goldstein, S.A., 2009. A designer ligand
578 specific for Kv1.3 channels from a scorpion neurotoxin-based library. Proc Natl Acad Sci U S A 106,
579 22211-22216.
580 Tarcha, E.J., Chi, V., Munoz-Elias, E.J., Bailey, D., Londono, L.M., Upadhyay, S.K., Norton, K., Banks, A.,
581 Tjong, I., Nguyen, H., Hu, X., Ruppert, G.W., Boley, S.E., Slauter, R., Sams, J., Knapp, B., Kentala, D.,
582 Hansen, Z., Pennington, M.W., Beeton, C., Chandy, K.G., Iadonato, S.P., 2012. Durable pharmacological
583 responses from the peptide ShK-186, a specific Kv1.3 channel inhibitor that suppresses T cell mediators
584 of autoimmune disease. J Pharmacol Exp Ther 342, 642-653.
585 Toldi, G., Bajnok, A., Dobi, D., Kaposi, A., Kovacs, L., Vasarhelyi, B., Balog, A., 2013. The effects of Kv1.3
586 and IKCa1 potassium channel inhibition on calcium influx of human peripheral T lymphocytes in
587 rheumatoid arthritis. Immunobiology 218, 311-316.
588 Toth, A., Szilagyi, O., Krasznai, Z., Panyi, G., Hajdu, P., 2009. Functional consequences of Kv1.3 ion
589 channel rearrangement into the immunological synapse. Immunol Lett 125, 15-21.
590 Upadhyay, S.K., Eckel-Mahan, K.L., Mirbolooki, M.R., Tjong, I., Griffey, S.M., Schmunk, G., Koehne, A.,
591 Halbout, B., Iadonato, S., Pedersen, B., Borrelli, E., Wang, P.H., Mukherjee, J., Sassone-Corsi, P., Chandy,

592 K.G., 2013. Selective Kv1.3 channel blocker as therapeutic for obesity and insulin resistance. Proc Natl
593 Acad Sci U S A 110, E2239-2248.
594 Utsunomiya, I., Yoshihashi, E., Tanabe, S., Nakatani, Y., Ikejima, H., Miyatake, T., Hoshi, K., Taguchi, K.,
595 2008. Expression and localization of Kv1 potassium channels in rat dorsal and ventral spinal roots. Exp
596 Neurol 210, 51-58.
597 Varga, Z., Gurrola-Briones, G., Papp, F., Rodriguez de la Vega, R.C., Pedraza-Alva, G., Tajhya, R.B., Gaspar,
598 R., Cardenas, L., Rosenstein, Y., Beeton, C., Possani, L.D., Panyi, G., 2012. Vm24, a natural
599 immunosuppressive peptide, potently and selectively blocks Kv1.3 potassium channels of human T cells.
600 Mol Pharmacol 82, 372-382.
601 Varga, Z., Hajdu, P., Panyi, G., 2010. Ion channels in T lymphocytes: an update on facts, mechanisms and
602 therapeutic targeting in autoimmune diseases. Immunol Lett 130, 19-25.
603 Varga, Z., Juhasz, T., Matta, C., Fodor, J., Katona, E., Bartok, A., Olah, T., Sebe, A., Csernoch, L., Panyi, G.,
604 Zakany, R., 2011. Switch of voltage-gated K+ channel expression in the plasma membrane of
605 chondrogenic cells affects cytosolic Ca2+-oscillations and cartilage formation. PLoS One 6, e27957.
606 Varghese, A., Tenbroek, E.M., Coles, J., Jr., Sigg, D.C., 2006. Endogenous channels in HEK cells and
607 potential roles in HCN ionic current measurements. Prog Biophys Mol Biol 90, 26-37.
608 Vianna-Jorge, R., Oliveira, C.F., Garcia, M.L., Kaczorowski, G.J., Suarez-Kurtz, G., 2003. Shaker-type Kv1
609 channel blockers increase the peristaltic activity of guinea-pig ileum by stimulating acetylcholine and
610 tachykinins release by the enteric nervous system. Br J Pharmacol 138, 57-62.
611 Wang, H., Kunkel, D.D., Schwartzkroin, P.A., Tempel, B.L., 1994. Localization of Kv1.1 and Kv1.2, two K
612 channel proteins, to synaptic terminals, somata, and dendrites in the mouse brain. J Neurosci 14, 4588-
613 4599.
614 Wulff, H., Calabresi, P.A., Allie, R., Yun, S., Pennington, M., Beeton, C., Chandy, K.G., 2003. The voltage-
615 gated Kv1.3 K(+) channel in effector memory T cells as new target for MS. J Clin Invest 111, 1703-1713.

Xie, G., Harrison, J., Clapcote, S.J., Huang, Y., Zhang, J.Y., Wang, L.Y., Roder, J.C., 2010. A new Kv1.2 channelopathy underlying cerebellar ataxia. J Biol Chem 285, 32160-32173.

You, M.H., Song, M.S., Lee, S.K., Ryu, P.D., Lee, S.Y., Kim, D.Y., 2013. Voltage-gated K+ channels in adipogenic differentiation of bone marrow-derived human mesenchymal stem cells. Acta Pharmacol Sin 34, 129-136.

Yu, S.P., Kerchner, G.A., 1998. Endogenous voltage-gated potassium channels in human embryonic kidney (HEK293) cells. J Neurosci Res 52, 612-617.

Zhao, N., Dong, Q., Du, L.L., Fu, X.X., Du, Y.M., Liao, Y.H., 2013. Potent suppression of Kv1.3 potassium channel and IL-2 secretion by diphenyl phosphine oxide-1 in human T cells. PLoS One 8, e64629.

Zhu, G., Zhang, Y., Xu, H., Jiang, C., 1998. Identification of endogenous outward currents in the human embryonic kidney (HEK 293) cell line. J Neurosci Methods 81, 73-83.